Molecular Modeling and Site-Directed Mutagenesis Studies of a Phorbol Ester-Binding Site in Protein Kinase C

Shaomeng Wang,[†] Marcelo G. Kazanietz,[‡] Peter M. Blumberg,[‡] Victor E. Marquez,[†] and G. W. A. Milne*,[†]

Laboratories of Medicinal Chemistry and of Cellular Carcinogenesis and Tumor Promotion, Division of Basic Sciences, National Cancer Institute, NIH, Bethesda, Maryland 20892

Received June 2, 1995[⊗]

The protein kinase C (PKC) binding site used by PKC activators such as phorbol esters and diacylglycerols (DAGs) has been characterized by means of molecular modeling and site-directed mutagenesis studies. Based upon a NMR-determined solution structure of the second cysteine-rich domain of PKC α, molecular modeling was used to study the structures of the complexes formed between the PKC receptor and a number of PKC ligands, phorbol esters, and DAGs. Site-directed mutagenesis studies identified a number of residues important to the binding of phorbol esters to PKC. Analysis of the molecular modeling and mutagenesis results allows the development of a binding model for PKC ligands for which the precise binding nature is defined. The calculated hydrogen bond energies between the protein and various ligands in this binding model are consistent with their measured binding affinities. The binding site for phorbol esters and DAGs is located in a highly conserved, hydrophobic loop region formed by residues 6−12 and 20−27. For the binding elements in phorbol esters, the oxygen at C_{20} contributes most to the overall binding energy, and that at C_3 plays a significant role. The oxygen atom at C_{12} is not directly involved in the interaction between phorbol esters and PKC. Our results also suggest that the oxygens at C_9 and C_{13} are involved in PKC binding, while the oxygen at C_4 is of minimal significance. These results are consistent with known structure−activity relationships in the phorbol ester family of compounds. Comparisons with the X-ray structure showed that although the X-ray data support the results for oxygens at C_3, C_{12}, and C_{20} of phorbol esters, they suggest different roles for oxygens at C_4, C_9, and C_{13}. Several factors which may contribute to these discrepancies are discussed.

Introduction

Protein kinase C (PKC), a family of at least nine closely related isozymes, is intimately involved in the regulation of a variety of cellular functions such as gene expression, cellular growth, and differentiation.[1−6] Most PKC isozymes are activated by lipids, in particular by diacylglycerol (DAG), in either a calcium-dependent or -independent manner.[1−4,7] PKC has also been identified as a major cellular receptor for the phorbol esters,[1,8] potent tumor-promoting diterpene derivatives from plants. Although DAG is thought to be the endogenous ligand, its binding to PKC is weak, and the activation it provides is transitory.[4,7] Phorbol esters such as phorbol 12,13-dibutyrate (PDBU) and phorbol 12-myristate 13-acetate (PMA) compete with the DAG for the same binding site and can activate PKC with an affinity at least 3 orders of magnitude higher[8] than that of DAG. An understanding of the interaction of activators with PKC is fundamental to studies of the mechanism of the activation of PKC and necessary for the rational design of novel PKC ligands. In the absence of information concerning the three-dimensional structure of the enzyme, much work has been carried out aimed at defining a common pharmacophore involved in the binding of different ligands to PKC.[9−14] All the PKC isozymes contain two cysteine-rich domains, either of which is sufficient for competent binding of PDBU. Recently, the three-dimensional structure of the second cysteine-rich domain of the isozyme PKC_α was determined by NMR spectroscopy,[15,16] and these data provided an opportunity to evaluate the binding of various ligands by this domain. This paper presents the results of molecular modeling and site-directed mutagenesis on the determination of the phorbol ester-binding site in this domain of PKC. These results facilitate a detailed analysis of the interactions between the receptor and various ligands.

Materials and Methods

Structure of the Second Cysteine-Rich Domain of PKC_α. The solution structure of the second cysteine-rich domain of PKC_α (residues 92−163) was determined by Hommel et al.[15] and Ichikawa et al.[16] using homonuclear two-dimensional and ^{15}N-edited three-dimensional NMR experiments and was used in the calculations described in this paper. The N-terminal residues 92−101 and the C-terminal residues 153−163 were found to be unstructured,[15] and since they are not required for the high-affinity binding of PKC to phorbol esters and other PKC ligands,[17] they were not included in the molecular modeling study. The segment[18] from His_{102} (renumbered as His_1) to Cys_{152} (Cys_{50}), as shown in Figure 1, was studied.

Molecular Modeling. All molecular modeling and molecular dynamics studies were carried out using the QUANTA molecular modeling package (Version 3.3)[19] with CHARMm 2.2 force field parameters[20] running on a Silicon Graphics IRIS Indigo workstation or a standalone version of CHARMm running on a Convex supercomputer. Energy minimizations were typically computed with 30 000 iterations of an adjusted basis Newton−Raphson algorithm. Dynamics simulations were carried out on structures *in vacuo* using a distance-dependent dielectric constant ($D = r$) or in a system hydrated with *ca.* 500 explicit water molecules. In a typical molecular dynamics simulation, the system is first heated to 300 K over a 10 ps time period and then equilibrated at 300 K for 10 ps and finally allowed to undergo dynamics simulation at 300 K

[†] Laboratory of Medicinal Chemistry.
[‡] Laboratory of Cellular Carcinogenesis and Tumor Promotion.
[⊗] Abstract published in *Advance ACS Abstracts,* April 15, 1996.

S0022-2623(95)00403-1

```
                1         10        20        30        40        50
bovine α  HKFKIHTYGS PTFCDHCGSL LYGLIHQGMK CDTCDMNVHK QCVINVPSLC
rat    β  HKFKIHTYSS PTFCDHCGSL LYGLIHQGMK CDTCMMNVHK RCVMNVPSLC
rat    γ  HKFRLHSYSS PTFCDHCGSL LYGLVHQGMK CSCCEMNVHR RCVRSVPSLC
rat    δ  HRFKVYNYMS PTFCDHCGTL LWGLVKQGLK CEDCGMNVHH KCREKVANLC
rat    ε  HKFGIHNYKV PTFCDHCGSL LWGLLRQGLQ CKVCKMNVHR RCETNVAPNC
mouse  η  HKFNVHNYKV PTFCDHCGSL LWGIMRQGLQ CKICKMNVHI RCQANVAPNC
mouse  θ  HRFKVYNYKS PTFCEHCGTL LWGLARQGLK CDACGMNVHH RCQTKVANLC

mouse  ζ  HLFQAKRFNR GAYCGQCSER IWGLSRQGYR CINCKLLVHK RCHVLVPLTC
```

Figure 1. Sequence of the second cysteine-rich domain of different PKC isoforms. Conserved residues are in boldface.

for 30 ps or longer. During the simulations, snapshots are taken and subsequently analyzed to determine the behavior of the molecules.

Two zinc atoms coordinate with a total of six cysteine and two histidine residues in this domain and form the integral part of the protein structure. Each of these two zinc atoms was found to coordinate with four atoms in a tetrahedral manner: three sulfur atoms on three cysteine residues with a distance of 2.1 Å and one nitrogen on one histidine with a distance of 1.9 Å according to the NMR structure.[15] NMR distance constraints were introduced in all the calculations to restrain the bonds between zinc atoms and these eight residues. No other constraints were used in the calculations for both the protein and the ligands studied.

PKC Bioassay. Binding affinity to PKC was determined by measuring the competitive displacement of [20-^{3}H]phorbol 12,13-dibutyrate from the isozyme PKC$_\alpha$ by the various compounds assayed. The details of this method have been described previously.[21]

Site-Directed Mutagenesis Experiments. The details of the methods used in site-directed mutagenesis experiments have been described elsewhere.[22] Briefly, site-directed mutagenesis was performed with the unique site elimination (USE) system (Pharmacia, Piscataway, NJ), using the pGEXdelta plasmid as the template. The Pstl site in the vector was eliminated by using the Pstl/SacII pGEX USE primer from the same company. Mutant plasmids were selected by restriction analysis, as described by the manufacturer and confirmed by sequencing using the dideoxy chain termination method. The mutant plasmids were used to express the corresponding mutant GST-fusion proteins, which were purified with glutathione-Sepharose 4B beads. The binding affinities of these mutants to PDBU were determined using the procedure described above.

Results and Discussion

3D Structure of the Second Cysteine-Rich Domain of PKC$_\alpha$. All PKC isozymes have two functionally distinct segments, a carboxyl-terminal kinase domain and an amino-terminal regulatory domain. The regulatory domain in PKC contains two cysteine-rich domains each of about 50 amino acids, including a sequence: $HX_{12}CX_2CX_{13,14}CX_2CX_4HX_2CX_7C$, where H is histidine, C is cysteine, and X are variable residues. These cysteine-rich domains are also called "zinc fingers" since each of them is found to coordinate with two zinc ions.[23,24] It has been demonstrated that the phorbol ester- and DAG-binding site is located within these two domains, either of which is sufficient for high-affinity phorbol ester binding.[17,25−28] Accordingly, we chose to study the second of these zinc fingers, whose sequence is shown in Figure 1.

The topology of this domain in the NMR solution structure,[15] as shown in Figure 2, can be described as two antiparallel β sheets. A helix at the C-terminal end of the chain follows the last β strand and folds back to the N-terminus underneath the major β sheet.[15,16] Two zinc ions, each coordinated by one histidine and three cysteine residues, are critical for the integrity of the overall scaffold, but the loops from His$_6$ to Phe$_{13}$ and

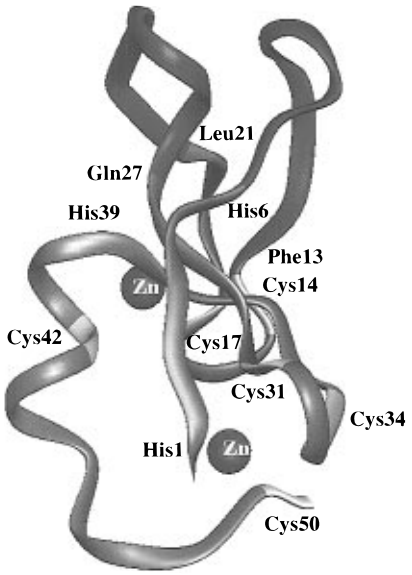

Figure 2. NMR-determined solution structure of PKC$_\alpha$.

Leu$_{21}$ to Gln$_{27}$ are largely independent of the zinc atoms and are fairly flexible, as can be seen from Figure 2. The structure of this region is well defined except for residues Gly$_8$, Ser$_9$, Gly$_{23}$, Leu$_{24}$, Ile$_{25}$, His$_{26}$, and Gln$_{27}$.

Molecular dynamics simulations were employed to investigate the stability and flexibility of this domain. The NMR structure of this region,[15] shown in Figure 2, was hydrated in a water sphere of 30 Å diameter and this system was energy-minimized in 30 000 steps of adjusted-basis Newton−Raphson calculation until convergence, defined as an energy gradient of ≤0.0001 kcal/Å, was achieved. The resulting energy-minimized structure was used as a starting point for molecular dynamics simulations. In the first experiment, the structure was heated to 300 K over a 10 ps period, equilibrated at 300 K for 10 ps, and then simulated for 30 ps. During the simulation phase, snapshots were taken at intervals of 0.3 ps, giving a total of 100 structures. In a second experiment, the entire process was repeated with a final temperature of 1000 K. The results of the two runs were then compared by taking every tenth structure and computing the rms deviation between its backbone heavy atoms and those of the structure before the simulation. Figure 3 shows a number of structures from the 300 K simulation superimposed upon one another and reveals that two loops, residues 6−13 and 21−27, clearly have a high degree of mobility with respect to the backbone of the remainder of the protein, which is relatively rigid. Aside from the atoms of these two loops, there is little movement of atoms in the 300 K simulations, showing that overall the structure is stable. But simulation at 1000 K shows a good deal of shifting of all heavy atoms (rms = 4.801 Å), with the displacement concentrated in residues 6−13 and 21−27 (rms = 5.530 Å) rather than in the other residues (rms = 3.387 Å), indicating that the two loops formed by residues 6−13 and 21−27 are more flexible than the remainder of the chain. This observation is consistent with the NMR results which revealed a lack of NOE data for these residues, on account of their relative mobility.[15,16]

Phorbol Ester-Binding Sites. PKC consists of at least nine isoforms. Except for PKC$_\zeta$ and PKC$_\lambda$, which represent an atypical PKC subclass, all the isoforms have high binding affinity for phorbol esters such as

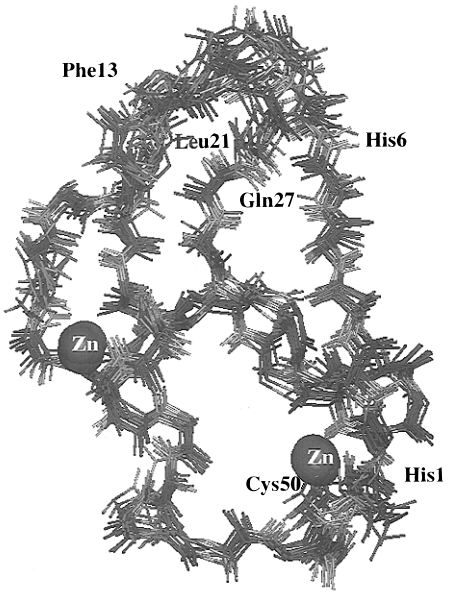

Figure 3. Molecular dynamics simulations (300 K) of the second cysteine-rich domain of PKC_α. Note the marked flexibility in the His_6−Gln_{27} region.

PDBU.[29] Analysis of the consensus sequences in these isoforms (Figure 1), in conjunction with the NMR solution structure, reveals some useful information regarding the location of the binding site in the protein. As can be seen from Figure 1, a number of the residues in the domain are conserved. Six cysteines (Cys_{14}, Cys_{17}, Cys_{31}, Cys_{34}, Cys_{42}, and Cys_{50}) and two histidines (His_1 and His_{39}), which are coordinated with the two zinc atoms, are highly conserved and are critical to the overall structure of the protein. All of these except Cys_{50} have been found to be essential for high-affinity phorbol ester binding.[22]

Several conserved hydrophobic residues were found to contribute to hydrophobic cores in the zinc finger and are therefore important to its overall folding. Such residues include Phe_3, Leu_{20}, Met_{29} (Leu_{29} in PKC_δ, PKC_ϵ, PKC_η, and PKC_θ, Tyr_{29} in PKC_ζ), Met_{36} (Leu_{36} in PKC_ζ), Val_{38}, and Val_{46}. Site-directed mutagenesis studies[22] have confirmed the absolute requirement of Phe_3, Leu_{20}, and Val_{38} and have also shown that Val_{46} is not required for high-affinity binding to phorbol esters. This is consistent with the observation that the first 43-residue peptide (His_1−Val_{43}) is capable of phorbol ester binding[30] and suggests that the C-terminus is not likely to be a part of the phorbol ester-binding site. Gln_{27} and Asn_{37} are both conserved, their side chains buried inside the protein, and form a number of hydrogen bonds with other residues. They are thought to be important to the overall scaffold and are thus crucial to high-affinity phorbol ester binding, as has been confirmed by mutagenesis studies.[22]

A number of conserved hydrophobic residues are not involved in the internal structure of the protein but rather are exposed to external solvent.[15,16] Such residues include Tyr_8, Phe_{13}, Leu_{20}, Tyr_{22} (Trp_{22} in PKC_δ, PKC_ϵ, PKC_η, and PKC_θ), Leu_{24}, and Ile_{25}. It was found from the NMR structure of the cysteine-rich domain in solution that these residues are grouped together and form a hydrophobic "cap". Mutation to Gly of Trp_{22} (corresponding to Tyr_{22} in PKC_α) in PKC_δ results in loss of the PKC/phospholipid association,[31] suggesting that this region is involved in PKC/phospholipid interaction. When DAG binds to PKC, the hydrophobic portion of the DAG is associated with the phospholipid membrane.[2,3] Phospholipid is known to be important to the binding of PKC to DAG[1,2] and to phorbol esters, as well as to the activation of PKC.[1,2,4] In membrane-binding proteins such as phospholipase A_2, an exposed hydrophobic surface is required for the protein to form an interfacial binding surface with the lipid.[32] All of this evidence suggests that DAG and PDBU both bind to the same hydrophobic region of PKC and the best candidate regions, consistent with the mutation data, are either one or both of the loops formed by residues 6−13 and 21−27. This is the same region which, as noted above, is particularly flexible, as indicated by the NMR data and the molecular dynamics simulations described above.

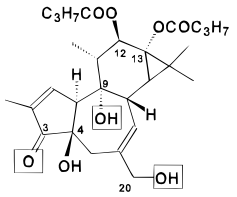

Phorbol-12,13-dibutyrate (PDBU)

Numerous structure−activity studies[9,11,13,14] have argued for a three-point pharmacophore as the minimum requirement for any ligand to compete with DAG for the active site of PKC. In PDBU, Rando and coworkers[13,14] have suggested that this pharmacophore consists of two oxygens of the C_3 carbonyl and C_9 hydroxyl, functioning as hydrogen bond acceptors, and the hydroxyl group at C_{20}, serving as a hydrogen bond donor. Previous studies have indicated that the hydroxyl group at C_4[10] and the ester group at C_{13}[33] are also significant to the binding affinity of phorbol esters to PKC. Although these groups may not be as important as the primary three points (C_3, C_9, and C_{20}), their deletion does result in reduced binding affinities. The ester group at C_{12} was found to have no effect on the binding affinity of phorbol esters to PKC.[34] The high binding affinity to PKC for compounds with at least the three-point pharmacophore suggests that highly optimized hydrogen bonds are formed between these atoms and the enzyme. This reasoning was used in our earlier study[35] of a pseudoreceptor model which allowed a plausible estimation of binding energies. The phorbol ester pharmacophore was therefore used to help determine the precise binding features between phorbol esters and the second cysteine-rich domain of PKC. Provided that ligands do not differ in overall hydrophobicity or orientation of their hydrophobic domain, the ability to interact with PKC *via* hydrogen bonds is perhaps the most important factor responsible for their different binding affinities. Accordingly, the total hydrogen bond energy between a ligand and the PKC was used in this study as a parameter with which to judge how well a ligand binds to PKC.

In order to interact with the phorbol skeleton by means of a three-point pharmacophore, the binding site must have, at a minimum, three complementary hydrogen bond donors/acceptors in a geometry that is consistent with formation of strong hydrogen bonds to the three pharmacophoric atoms of the phorbol skeleton. Docking experiments followed by energy minimization and hydrogen bond analysis revealed the three most

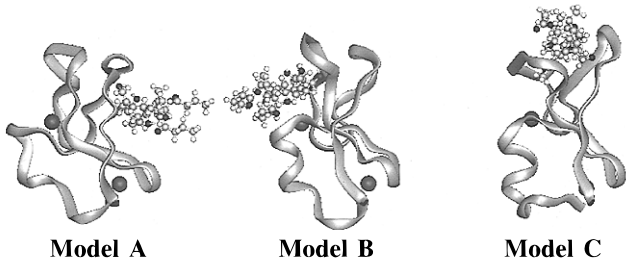

Figure 4. Three possible PKC/PDBU binding models (models A−C).

promising binding sites, shown in Figure 4, termed models A−C. Models A and B are located on either side of these two loops, while model C resides in between the two loops, formed by His_6−Phe_{13} and Leu_{21}−Gln_{27}. More detailed studies were carried out to select the preferred binding model and to study the details of the interaction between the ligand and the PKC.

Model A, as shown in Figure 4, was based upon a postulate first proposed by Hommel,[15] involving residues Lys_4, Pro_{11}, Phe_{13}, Gln_{27}, and Lys_{30}. To test this site, a minimized structure of PDBU was docked in it and the entire system was minimized to give the enzyme−ligand complex shown in Figure 4. This complex contains seven hydrogen bonds between the ligand and the enzyme, and the total energy of these hydrogen bonds was calculated as −9.68 kcal/mol. The C_3 carbonyl oxygen interacts with the backbone −NH of Phe_{13} and the side chain amino group of Lys_{30}. The oxygen at C_9 forms one hydrogen bond with the side chain amino group of Lys_4. Interestingly, this same amino group interacts with the carbonyl oxygen of the ester at C_{13} in PDBU. The hydroxyl group at C_{20} of the PDBU acts not only as a hydrogen bond donor, interacting with the backbone carbonyl oxygen of Pro_{11}, but also as an acceptor, forming a very strong hydrogen bond with the side chain amino group of Gln_{27}. Model A also appears to have a role for the hydroxyl group at C_4 of the PDBU which functions as a hydrogen bond donor, interacting with the backbone carbonyl oxygen of Pro_{11}. This model is fully consistent with previously established views of the pharmacophore in PDBU, but a careful examination of each of the enzyme−ligand hydrogen bonds reveals them all to be suboptimal in terms of geometry and thus stability. The average energy of these hydrogen bonds is only −1.35 kcal/mol, a figure that is inconsistent with the high binding affinity of PDBU to PKC, which requires optimal interactions between the ligand and the receptor. For this reason, model A must be regarded as doubtful.

In model B, as shown in Figure 4, the ligand is attached to the enzyme by means of seven hydrogen bonds involving five residues, Tyr_{22}, Leu_{24}, Ile_{25}, Lys_{40}, and Gln_{41}. There is a distinct cavity on the enzyme surface at this site and ample space in which to accommodate the ligand. In the energy-minimized structure of this enzyme−ligand complex, with a total hydrogen bond energy of −21.44 kcal/mol, the oxygen of the C_3 carbonyl interacts with the backbone −NH groups of Leu_{24} and Ile_{25}, forming hydrogen bonds with energies of −2.22 and −3.21 kcal/mol, respectively. The C_9 hydroxyl, acting as a hydrogen bond acceptor, forms a strong hydrogen bond with the backbone −NH of Lys_{40}, and the C_{20} hydroxyl group, acting as a hydrogen bond donor, forms a strong hydrogen bond with the backbone oxygen of Tyr_{22}. The carbonyl oxygen of the ester at C_{13} forms two strong hydrogen bonds with the backbone −NH and the side chain amino group of Gln_{41}. The total energy of these two hydrogen bonds is −5.27 kcal/mol. The carbonyl oxygen of the ester at C_{12} also plays a role by forming a strong hydrogen bond (−3.22 kcal/mol) to the side chain amino group of Gln_{41}, but this model appears to have no role for the hydroxyl group at C_4 of the PDBU. Model B has much stronger protein−ligand interactions than are possessed by model A. All the crucial binding points in PDBU appear optimally attached to the protein in model B, a better alternative.

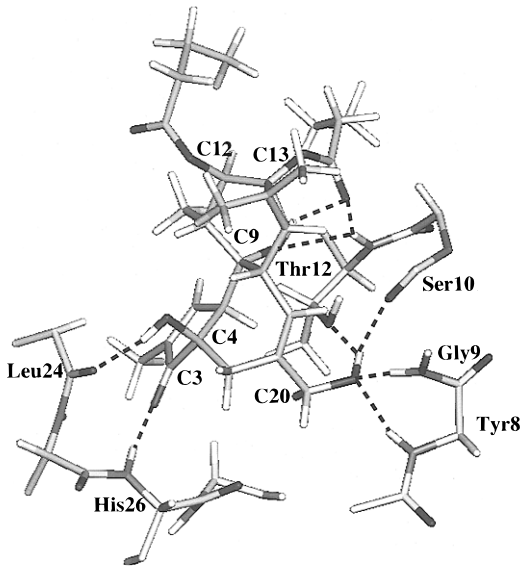

Figure 5. Hydrogen bonds formed between PKC and PDBU in model C.

Models A and B are on either side of the loops formed by residues 6−13 and 21−27, as shown in Figures 2 and 4. As has been seen from NMR and dynamics simulation data, these two loops are relatively mobile, and it is reasonable to investigate whether the ligand could lodge between them.

Accordingly, in model C (Figures 4 and 5), PDBU was docked into this site, and the complex was minimized to give a structure which is shown in part in Figure 5. This complex contains eight strong hydrogen bonds between the ligand and Tyr_8, Gly_9, Ser_{10}, Thr_{12}, Leu_{24}, and His_{26} of the protein, and the associated hydrogen bond energy is calculated as −18.72 kcal/mol. The carbonyl oxygen at C_3 of the PDBU forms a hydrogen bond with the backbone −NH of His_{26}, contributing −3.23 kcal/mol. The hydroxyl group at C_9, functioning as a hydrogen bond acceptor, forms a weak hydrogen bond with the backbone −NH of Thr_{12} with an energy of −0.65 kcal/mol. The hydroxyl at C_{20} behaves as a hydrogen bond donor, forming two hydrogen bonds, one with the side chain hydroxyl of Thr_{12} and the other with the backbone oxygen of Ser_{10}. It also behaves as an acceptor, interacting with the backbone −NH groups of Tyr_8 and Gly_9. All told, the C_{20} hydroxyl contributes, *via* these four hydrogen bonds, −7.26 kcal/mol to the whole complex and is the most important point in the pharmacophore. The C_4 hydroxyl group of PDBU, in this model, functions as a hydrogen bond donor, interacting with the backbone oxygen of Leu_{24} with a hydrogen bond energy of −3.97 kcal/mol, and the

Table 1. Total Hydrogen Bond Energies (kcal/mol) for Binding of PDBU to PKC$_\alpha$ in Models A−C

model		
A	B	C
−9.68	−21.44	−18.72

carbonyl oxygen of the ester at C_{13} forms a hydrogen bond with the backbone −NH of Thr_{12}. In this model, the ester at C_{12} is projected outside the body of the enzyme and does not form any hydrogen bond to it. Further evidence emerging from an X-ray analysis[36] showed that the binding site indicated by model C was in fact correct, as is discussed below.

Comparison of Models A−C. Examination of the details of these three models quickly reveals model A to be distinctly inferior to either of the alternatives. This is due primarily to the absence in model A of geometrically optimal hydrogen bonds. Because of this, the total enzyme−ligand hydrogen bond energy in this model (Table 1) is only −9.68 kcal/mol—approximately one-half that of models B and C. On the basis of total hydrogen-bonding energy, model B would appear to be some 21.44 − 18.72 = 2.72 kcal/mol better than model C. The total hydrogen bond energy from model B however includes −3.22 kcal/mol from the interaction involving the carbonyl oxygen of the ester at C_{12}, which is known to have no significant contribution to the high binding affinity of PDBU to PKC. Further, models A and C allow a hydrogen bond from PKC to the C_4 hydroxyl of PDBU indicating its significance to the PDBU/PKC interactions, consistent with experimental results.[9−14] The preponderance of evidence available at this point thus suggests model C to be the best of the alternatives.

Different PKC$_\alpha$ Ligands. There is abundant information available concerning the structure−activity relationships of phorbol esters, as well as other classes of PKC ligands.[9−14] A correct binding model must be capable of distinguishing ligands with high binding affinities from those with weak binding affinities. Therefore, a number of phorbol esters analogues and diacylglycerols were investigated for their detailed interactions with PKC$_\alpha$ within each of these three models. Their chemical structures are shown, and the results are summarized in Table 2.

The 4-methyl ether of PDBU binds to PKC with a binding affinity 1100 times less than that of PDBU itself. When the 4-methyl ether was docked in models A−C, the total hydrogen bond energies were calculated to be −6.28, −17.49, and −12.32 kcal/mol, respectively. The complex formed between the 4-methyl ether and model B, shown here, reveals hydrogen bonds between the C_3 carbonyl and the backbone NH of Leu_{24} and between the C_{20} hydroxyl group and the carbonyl of Tyr_{22}. The C_9 hydroxyl is hydrogen bonded to the backbone NH of Lys_{40}, and the carbonyl of the ester at C_{13} is hydrogen bonded to both the backbone NH group and the side chain of Gln_{41}.

In model C, the C_3 carbonyl of the 4-methyl ether of PDBU is hydrogen bonded to His_{26} and the hydroxyl at C_{20} hydrogen bonds as an acceptor to the backbone NH group of both Tyr_8 and Gly_9 and as a donor to the backbone carbonyl group of Thr_7. Both the hydroxyl at C_9 and the carbonyl oxygen of the C_{13} ester function as acceptors, forming hydrogen bonds to the NH group of Thr_{12}. It was found that in model C, the methoxyl at C_4 of this ligand is not hydrogen bonded to the protein.

Table 2. Experimentally Deduced Binding Affinity (K_i) and Calculated Binding Energies of Different Ligands to PKC$_\alpha$ in Models A−C[a,d]

ligand	relative binding affinity	ref	HB energy (kcal/mol) model A	model B	model C
PDBU	1	*a*,29	−9.68	−21.44	−18.72
4-deoxy PDBU	5	*b*	−9.11	−18.30	−14.92
(*S*)-DAG	1500	29		−12.03	−13.00
PDBU 4-methyl ether	1100	34	−6.28	−17.49	−12.32
PDBU 20-methyl ether	>7000	*c*	−9.41	−11.76	−10.57
4α-hydroxy PDBU	>10 000	*b*	−11.36	−18.90	−9.09
20-deoxy PDBU	>7000	*c*	−8.50	−11.66	−7.89
(*R*)-DAG	inactive	38,39		−9.70	−6.11

[a] Binding affinity expressed relative to that of PDBU = 1. [b] Fürstenberger, G.; Hecker, E. On the Active Principles of the Spurge Family (*Euphorbiaceae*). XI. [1] The Skin Irritant and Tumor Promoting Diterpene Esters of *Euphorbia tirucalli* L. Originating from South Africa. *Z. Naturforsch.* **1985**, *400*, 631−646. [c] Thielmann, H. W.; Hecker, E. Beziehungen zwischen der Struktur von Phorbolderivaten und ihren Entzundlichen und Tumorpromotierenden Eigenschaften. In *Fortschritte der Krebsforschung*; Schmit, C. G., Ed.; Schattauer: Stuttgart, New York; Vol. VII, pp 171−179. [d] Relative affinities for PDBu derivatives were estimated from experimental data for the corresponding derivatives of other phorbol esters.

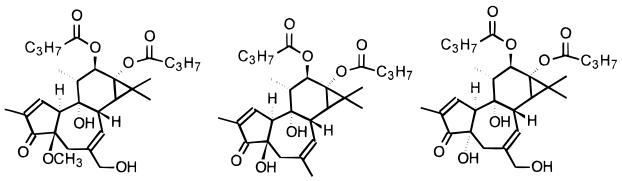

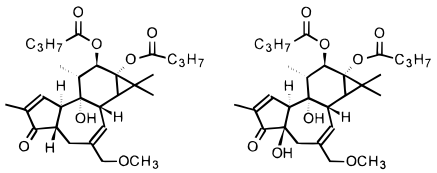

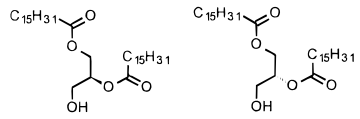

The difference in the hydrogen bond energy between the 4-methyl ether of PDBU and PDBU with respect to model C is 6.40 kcal/mol, easily enough[37] to account for the 1100-fold difference in binding affinity between these two ligands. In model B in contrast, the hydrogen bond energy difference between these two ligands is only 3.95 kcal/mol and almost all of this (−3.44 kcal/mol) arises from a hydrogen bond involving the C_{12} carbonyl oxygen—an interaction which is known to be absent from the PDBU−PKC$_\alpha$ system. The data on the 4-methyl ether of PDBU therefore are in favor of model C. Methylation of the 4-hydroxyl group in PDBU destroys the ability of the hydroxyl group to behave as a hydrogen bond donor.

The 4-epimer of PDBU, 4α-hydroxy PDBU, fails to bind to PKC,[9] and this finding has not found an explanation in terms of any of the pharmacophores postulated previously.[9,11,13,14] This molecule was docked in each of the three binding models, and the hydrogen

bond energies between the ligand and the enzyme for the minimized complexes were found to be −11.36 kcal/mol in model A, −18.90 kcal/mol in model B, and −9.09 kcal/mol in model C. In model A there are six relatively strong and several weak hydrogen bonds formed between the ligand and the enzyme, and the overall hydrogen bond energy is −1.68 kcal/mol more than that for PDBU. This suggests that the 4-epimer should bind more effectively than PDBU itself, a result that is contradicted by experiment. In model B, the 4-epimer forms nine relatively strong hydrogen bonds, as well as several weak hydrogen bonds, with the enzyme. The oxygen of the C_3 carbonyl forms a hydrogen bond with the backbone −NH of Leu_{24}, and the 4α-hydroxyl group behaves as both a hydrogen bond acceptor, to the backbone −NH groups of Ile_{25} and His_{26}, and a hydrogen bond donor, to the backbone carbonyl oxygen of Gln_{27}. With three strong hydrogen bonds to the enzyme, this hydroxyl group contributes very significantly in model B to the binding of the 4-epimer to PKC. The C_9 hydroxyl group of this ligand forms two hydrogen bonds to the backbone −NH groups of Lys_{40} and Gln_{41}, and the carbonyl oxygen of the ester at C_{13} forms two hydrogen bonds with the side chain amino group and the backbone NH of Gln_{41}. With this array of nine strong hydrogen bonds, this ligand should possess a high affinity for PKC, but in fact, it fails entirely to bind to PKC and thus provides powerful evidence against the validity of model B. In the model C complex between PKC and the 4-epimer, only five hydrogen bonds can be found and the oxygen of the C_3 carbonyl and the 4-hydroxyl groups are not involved in any of them, presumably because the geometry of the system does not permit such hydrogen bonds to be formed. In this complex, the hydroxyl group at C_{20} of the ligand functions as a hydrogen bond acceptor, forming two hydrogen bonds to the backbone −NH groups of Tyr_8 and Gly_9, and also as a donor, forming a hydrogen bond to the side chain hydroxyl of Thr_7. The C_9 hydroxyl forms a hydrogen bond to the backbone −NH of Thr_{12}, and there is a weak hydrogen bond between the carbonyl oxygen of the C_{13} ester and the backbone NH group of Thr_{12}. In this model then, the failure of 4α-hydroxy PDBU to bind to PKC is explained, and this supports the validity of model C.

The interaction between PKC and the 20-methyl ether of PDBU was examined in the same way. In models A−C, the total hydrogen-bonding energy of this ligand was determined to be −9.41, −11.76, and −10.57 kcal/mol, respectively. Thus according to model A, the 20-methyl ether should bind as well as PDBU, while models B and C suggest that it should be a much poorer ligand than PDBU, with hydrogen bond energies −9.68 and −8.15 kcal/mol less, respectively. Experimentally, the 20-methyl ether of PDBU does not bind to PKC at all, and once again we have evidence against model A but support for models B and C. The repeated failure of model A to conform to experimental results led us at this point to remove it from further consideration.

The natural endogenous PKC ligands, the DAGs, are chiral compounds. The *S* isomers bind to PKC, while the *R* isomers fail to do so.[38,39] A probable active conformation for (*S*)-1,2-diacylglycerols has been proposed,[40] and this conformation was docked into each of the models B and C followed by the minimizations of the complexes. In model B, shown here, this ligand appears to bind fairly well to the PKC with a total hydrogen bond energy of −12.03 kcal/mol. The two carbonyl oxygens of the ligand are involved in three fairly strong hydrogen bonds to the backbone −NH groups of Leu_{24} and Lys_{40} and the side chain of Gln_{41}, and the primary hydroxyl group forms a strong hydrogen bond (−3.46 kcal/mol) with the backbone oxygen of Tyr_{22}. In model C, the ligand takes part in six hydrogen bonds, with a total energy of −13.00 kcal/mol. The carbonyl oxygen associated with C_2 forms a hydrogen bond (−2.57 kcal/mol) with the backbone −NH of His_{26}; the oxygen of the carbonyl at C_1 forms a hydrogen bond with the backbone −NH of Thr_{12}. The hydroxyl group in the ligand forms four hydrogen bonds. Behaving as a hydrogen bond donor, it interacts with the side chain of Thr_{12} and the backbone oxygen of Ser_{10}, and as an acceptor, it hydrogen bonds with the backbone −NH groups of Tyr_8 and Gly_9. Hydrogen bonds involving this hydroxyl contribute −6.81 kcal/mol to the total hydrogen-bonding energy which, this contribution notwithstanding, is at −13.00 kcal/mol still far below the value for PDBU (−18.72 kcal/mol). This indicates that, without even accounting for the additional entropy penalty that it will face, DAG will be a considerably poorer ligand than PDBU—an observation that is consistent with experimental results.

The starting conformation for (*R*)-DAG was derived from (*S*)-DAG by switching the primary hydroxyl group with the hydrogen atom on the chiral carbon. Then it was docked into the binding sites of models B and C, and the resulting complexes were minimized. Examination of the minimized complexes of the (*R*)-1,2-diacylglycerol/PKC in models B and C is instructive in that according to model B (five hydrogen bonds with a total energy of −9.70 kcal/mol), it should bind quite well to the enzyme, while model C (four hydrogen bonds, with a total energy of −6.11 kcal/mol) suggests that it should fail to bind. In fact, the (*S*)-1,2-diacylglycerols bind moderately well to PKC, but the *R* isomers do not,[40] and this supports model C over model B.

4-Deoxy PDBU, which should bind 5 times weaker than PDBU, was docked into the two binding sites B and C, and the complexes were then minimized. The total hydrogen bond energies between the ligand and the enzyme in the two minimized complexes were −18.30 and −14.92 kcal/mol, respectively. In both models B and C, 4-deoxy PDBU will have a lower affinity to PKC than PDBU, based upon −3.14 and −3.80 kcal/mol hydrogen bond energy differences between 4-deoxy PDBU and PDBU in these two models.

In summary, the data in Table 2 provide strong support for model C, which stands in contrast to the two other models. The total energy due to hydrogen bonding given by model C allows the ordering of the ligands in the correct order given by the binding affinities. The hydrogen-bonding energy for (*S*)-1,2-diacylglycerol was calculated to be −13.00 kcal/mol and is perhaps overstated. This compound and its *R* isomer are the only two ligands with significant flexibility, and they both will face entropy penalties as they attempt to bind to PKC. A conservative estimate[35] of the additional entropy penalty incurred by (*S*)-1,2-diacylglycerol as compared to PDBU when binding to PKC is 1.75 kcal/mol.

Table 3. Changes in Length of Hydrogen Bonds in the PDBU/PKC Complex during 300 K Dynamics Simulation

hydrogen bond (acceptor O, donor XH)	distance (Å)	
	acceptor−donor	acceptor−hydrogen
C_3=O···H−N (His_{26})	2.82 ± 0.10	1.91 ± 0.12
C_4−OH···O=C (Leu_{24})	2.75 ± 0.14	1.83 ± 0.15
C_{13}=O···H−N (Thr_{12})	2.85 ± 0.15	1.96 ± 0.18
C_{20}−O···H−N (Tyr_8)	3.00 ± 0.17	2.08 ± 0.19
C_{20}−O···H−N(Gly_9)	2.88 ± 0.17	2.00 ± 0.20
C_9−O···H−N (Thr_{12})	3.34 ± 0.20	2.59 ± 0.24
C_{20}−OH···O=C (Ser_{10})	2.87 ± 0.23	2.23 ± 0.38
C_{20}−OH···OH (Thr_{12})	2.84 ± 0.22	2.00 ± 0.30

Molecular Dynamics Simulations of the PKC/PDBU Complex *in Vacuo*. The foregoing data on different ligands, together with the site-directed mutagenesis experiments described below, all indicate that model C is the correct model and that the active site for PDBU binding is indeed located in the gap between the two loops 6−13 and 21−27 as shown in Figures 4 and 5. Molecular dynamics simulations were next employed to investigate the stability of this complex and to determine the contributions to the structure of the complex of each of the binding elements in PDBU and the corresponding residues on the protein.

A minimized complex structure of PDBU/PKC$_\alpha$ in the model C site was used as a starting structure for the dynamics simulations. The structure was slowly heated to 300 K in a period of 10 ps, equilibrated for 10 ps, and then subjected to molecular dynamics simulation for 100 ps at 300 K. Analysis of the resulting dynamics trajectory showed that during this simulation, PDBU stays tightly bound to the receptor, indicating that the complex is stable. Due to flexibility in both the ligand and the receptor, the hydrogen bonds formed between the ligand and the receptor show changes (summarized in Table 3) in their bond lengths and angles during the simulations. In this table, it can be seen that the last three hydrogen bonds (to Ser_{10} and Thr_{12}) stretch somewhat more than the others and are in fact relatively weak. Thus the C_9−O···−N (Thr_{12}) acceptor−hydrogen bond, with an average length of 2.59 ± 0.24 Å is easily stretched, and this is consistent with its low bond energy (0.77 kcal/mol). Likewise, two of the four hydrogen bonds to the C_{20} hydroxyl group are easily stretched, and in fact both of these are relatively weak; the system prefers to form one or the other but not both of these hydrogen bonds, and there is switching between these two bonds during the dynamics simulation. That such changes can occur is a source of the strength of the PDBU binding. As movement in the system stresses and begins to weaken a hydrogen bond, it can be replaced by an alternative hydrogen bond which may be either stronger or of similar strength.

A total of 11 snapshots of the system were taken at 0 ps and at the end of every 10 ps of simulation, and each of these structures was then minimized. Hydrogen bond analyses were carried out to the 11 minimized complexes, and the results are summarized in Table 4. The data show that the minimized complex structures derived from different snapshots have a similar total amount of hydrogen bond energy between the ligand and the receptor, with an average value of −18.51 ± 0.94 kcal/mol, indicative of strong interactions between the ligand and the receptor and of the stability of the complex. The hydroxyl group at C_{20} in PDBU contributes most significantly to the overall interaction, with

Table 4. Summary of the Total Hydrogen Bond Energy (kcal/mol) between PDBU and PKC$_\alpha$ in Model C for a Total of 11 Minimized Structures That Were Obtained from Molecular Dynamics Simulations and the Hydrogen Bond Energy Contributed from Each of the Binding Elements in PDBU

simulation time (ps)	total HB energy	HB energy between PKC$_\alpha$ and specific PDBU atoms				
		C_3 O	C_{20} OH	C_4 OH	C_9 OH	C_{13} O
0	−18.87	−3.20	−8.06	−3.99	−0.71	−3.58
10	−17.74	−1.90	−7.65	−3.95	−0.73	−3.51
20	−20.01	−2.13	−9.56	−4.05	−0.71	−3.56
30	−18.75	−2.93	−7.40	−4.01	−0.72	−3.68
40	−18.86	−2.84	−8.16	−3.51	−0.60	−3.74
50	−17.51	−2.08	−7.37	−3.96	−0.85	−3.24
60	−19.43	−2.05	−8.41	−4.01	−0.90	−4.05
70	−18.70	−1.89	−8.08	−3.98	−0.80	−3.96
80	−19.17	−1.84	−8.50	−4.01	−0.87	−3.95
90	−16.89	−1.26	−7.38	−4.01	−0.71	−3.54
100	−17.64	−1.50	−7.74	−4.08	−0.85	−3.48
			average			
	−18.51	−2.15	−8.03	−3.96	−0.77	−3.66
			SD			
	0.94	0.60	0.65	0.15	0.09	0.24

an average hydrogen bond energy of −8.03 kcal/mol, accounting for about 50% of the total hydrogen bond energy. This is consistent with the observation[42] that the elimination of the C_{20} hydrogen group in phorbol esters results in complete loss in the binding affinity to PKC. The molecular dynamics simulation results in Table 4 further show that the hydroxyl group at C_4 in PDBU has the second largest contribution to the total hydrogen bond energy, with an average value of −3.96 kcal/mol and a standard deviation of 0.15 kcal/mol. This hydroxy group functions as a hydrogen bond donor, forming a strong hydrogen bond with the carbonyl group of Leu_{24}. The carbonyl group of the ester at C_{13} in PDBU makes a very significant contribution to the binding, with a hydrogen bond energy of −3.66 kcal/mol, similar to that from the hydroxyl group at C_4. This carbonyl oxygen serves as a hydrogen bond acceptor, forming two hydrogen bonds with the backbone NH group and the side chain hydroxyl group of Thr_{12}. The carbonyl group at C_3 in PDBU contributes an average of −2.15 kcal/mol hydrogen bond energy. The hydroxyl group at C_9 in PDBU contributes the least to the total hydrogen bond energy, with an average value of −0.77 kcal/mol, but it forms a strong intramolecular hydrogen bond with the carbonyl group at C_{13} throughout the simulations, suggesting that it may play an important role in the binding by pinning the carbonyl group at C_{13} in PDBU in a conformation optimal for interaction with the receptor and so reducing the entropic loss in the binding. Because of this, the C_9 hydroxyl group of PDBU may be more important in the binding process than would be suggested by the −0.77 kcal/mol figure.

Molecular Dynamics Simulation of the PDBU/PKC Model in Water. In the studies described so far, we employed a distance-dependent dielectric constant to mimic the solvent environment in the dynamics simulations. This is a commonly used device to simplify the computation, but it is more useful, especially in the case of model C, to carry out simulations in a true water environment. In this way, it should be possible to obtain a model which can be used in direct comparisons with the X-ray-derived structure of the complex and in which potential problems arising from *in vacuo* calculations could be eliminated.

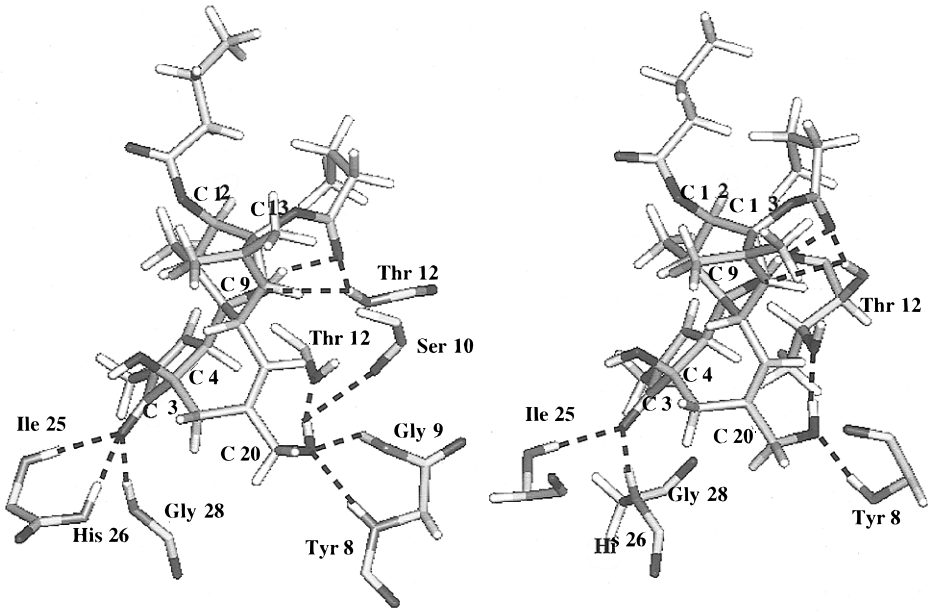

Figure 6. Molecular dynamics simulation trajectories at 50 and 150 ps of model C in water.

Table 5. Summary of the Total Hydrogen Bond Energy between PDBU and PKC_α for 15 Minimized Structures Obtained from 150 ps Molecular Dynamics Simulations in Water Beginning with the Complex Structure in Model C

simulation time (ps)	total HB energy (kcal)	HB energy between pKC_α and specific PDBU atoms				
		C_3 O	C_{20} OH	C_4 OH	C_9 OH	C_{13} OR
10	−21.00	−8.06	−7.18	0.00	−0.60	−5.17
20	−16.29	−2.97	−9.14	0.00	−0.73	−3.45
30	−18.52	−5.93	−7.43	−1.78	−0.80	−2.58
40	−21.54	−6.26	−7.63	−3.65	−0.78	−3.22
50	−21.28	−9.09	−8.62	0.00	−0.70	−2.87
60	−22.84	−8.99	−9.69	0.00	−0.63	−3.53
70	−19.39	−8.89	−7.68	0.00	−1.09	−1.73
80	−16.41	−5.64	−6.87	0.00	−0.79	−3.11
90	−13.77	−4.72	−5.13	0.00	−0.50	−3.42
100	−18.42	−9.79	−3.97	0.00	−1.01	−3.66
110	−15.29	−4.82	−6.51	0.00	−0.69	−3.27
120	−11.93	−1.67	−6.62	0.00	−0.85	−2.80
130	−18.66	−8.31	−6.31	0.00	−0.63	−3.42
140	−14.56	−5.38	−5.32	0.00	−0.94	−2.92
150	−17.53	−5.24	−7.58	0.00	−0.66	−4.05
		average				
	−17.83	−6.38	−7.05	−0.36	−0.76	−3.28
		SD				
	3.14	2.40	1.52	1.02	0.16	0.75

Accordingly, a 4 Å shell of *ca.* 500 water molecules was distributed evenly around the protein/ligand structure in model C, and the resulting system was subjected to molecular dynamics simulation for 150 ps at 300 K. Snapshots were made at the end of every 10 ps simulation, for a total of 15 structures. These 15 structures were then minimized in the water environment. An analysis of the hydrogen bonds in these structures is presented in Table 5. Two snapshots of the simulation trajectories at 50 and 150 ps are shown in Figure 6.

Examinations of the trajectories showed that the PKC_α and the PDBU remained tightly associated during the entire simulation. The average energy of hydrogen bonds between the ligand and the protein in these 15 structures is -17.83 ± 3.14 kcal/mol. The carbonyl oxygen at C_3 of the PDBU interacts consistently with the backbone NH groups of both Ile_{25} and His_{26}, and in some of the trajectories it is also involved in a hydrogen bond to the backbone NH of Gly_{28}. On average, hydrogen bonds to this oxygen of the PDBU contribute −6.38 kcal/mol to the total hydrogen bond energy. The C_4 hydroxyl group of PDBU was found to contribute only minimally to the overall hydrogen-bonding energy. This hydroxyl group formed hydrogen bonds to the protein in only two early trajectories of the 15 examined; it apparently has no significant interaction with the PKC_α after 50 ps of simulation. The C_{20} hydroxyl group, with an average hydrogen bond energy of −7.05 kcal/mol, remains the most important binding point in the PDBU. As a hydrogen bond acceptor, it binds to the backbone NH groups of both Tyr_8 and Gly_9, and acting as a hydrogen bond donor, it binds to either the backbone carbonyl group of Ser_{10} or the side chain hydroxyl of Thr_{12}, or, in some trajectories, to both. The hydroxyl group at C_9 of PDBU forms a weak hydrogen bond (average energy −0.76 kcal/mol) with the backbone NH of Thr_{12} and a strong intramolecular hydrogen bond, not with the PKC_α but with the carbonyl group at C_{13} of the PDBU. The oxygen of this carbonyl group forms a strong hydrogen bond with the backbone NH of Thr_{12}. The average energy of this hydrogen bond is −3.28 kcal/mol, making it the third most important binding point in PDBU. The carbonyl group of the C_{12} was found to be surrounded by solvent molecules and free of any significant interactions with the protein during the simulations.

Thus in an aqueous environment, binding of PDBU to PKC_α is primarily through the oxygens at C_3, C_{13}, and C_{20} of the PDBU. The oxygen at C_9 plays a complementary role, while that at C_4 has little significance in this process. The amino acid residues involved in the binding, in order of importance, are Ile_{25}, His_{26}, Tyr_8, Ser_{10}, Thr_{12}, Gly_9, and Gly_{28}.

Site-Directed Mutagenesis Studies. Site-directed mutagenesis studies were designed in order to identify the residues in this cysteine-rich domain that are important to the PKC/PDBU binding and provide direct experimental evidence relating to the phorbol ester-binding models that were derived from our modeling studies. All mutations were carried out on the PKC_δ isoform, and the detailed results have been published elsewhere.[22] PDBU binds to the second cysteine-rich

Table 6. Site-Directed Mutation[a]

residue[b]	consensus residue in PKC_δ	residue in PKC_α	K_D (nM)[c]
wild type			0.8 ± 0.
8	Try (238)	Tyr (109)	48.0 ± 3.00
11	Pro (241)	Pro (112)	100.0 ± 33.0
12	Thr (242)	Thr (113)	1.70 ± 0.30
13	Phe (243)	Phe (114)	0.90 ± 0.10
20	Leu (250)	Leu (121)	12 ± 1.8
21	Leu (251)	Leu (122)	>1000
22	Trp (252)	Tyr (123)	25.0 ± 3.00
24	Leu (254)	Leu (125)	>1000
27	Gln (257)	Gln (128)	>1000

[a] In every case, the designated residue was converted to Gly and the binding affinity of the mutant with PDBU was measured. [b] Residue numbering as in Figure 1 [c] PDBU binding.[22]

domain of PKC_δ with $K_d = 0.8$ nM, an affinity similar to that with which it binds to the corresponding domain of PKC_α ($K_d = 2.4$ nM). This similarity reflects the high conservation of the phorbol ester-binding domain among PKC isozymes and between species; indeed, binding of phorbol ester to PKC of nematodes and mice is virtually indistinguishable. Furthermore, the NMR solution structure of the phorbol ester-binding domain in PKC_α resembles the X-ray structure of the same domain in PKC_δ[36] very closely. Our mutagenesis studies were performed on PKC_δ, but the results obtained should be relevant to PKC_α. Here we summarize only the results for those residues directly related to the three models in our studies, as shown in Table 6.

Single mutation to Gly of any conserved residue in PKC can affect the PDBU binding capacity of the protein by (a) directly interfering in hydrogen bond formation to the ligand, (b) forcing a new folding pattern for the protein, or (c) affecting the lipid binding of the protein.

Mutation to Gly of either Tyr_8 and Pro_{11}, located in the loop formed by residues 6−13 and relevant to models A and C, results in partial loss of the PDBU binding affinity for the protein, suggesting the importance of these residues in PKC binding. Mutation of the conserved residues located on the loop formed by residues 21−27 also has a significant effect on the PKC/PDBU binding. Single mutations of Leu_{20} and Trp_{22} to Gly both result in a partial loss of the PDBU binding affinity for the protein, while the single mutations to glycine of residues Leu_{21}, Leu_{24}, and Gln_{27}, relevant to the proposed models B and C, all result in a complete loss of the PDBU binding with the protein. In the case of Gln_{27}, the side chain is buried inside the protein and forms a number of hydrogen bonds with both Gly_{23} and Val_{25}. This residue therefore appears to be important to the overall scaffold of the protein, and its mutation to Gly may result in a different folding for the protein, thus affecting the PDBU binding capability. For all the other residues in these two loops, as enumerated above, the side chains are extended toward to the surface of the protein and do not appear to participate directly in the protein folding. Thus, the partial or complete loss of the ability of the protein to bind to phorbol esters could be due to either the decrease in the protein's ability to associate with the lipid or to a significant change in the local conformation caused by the mutation, or the combination of both factors.

When hydrophobic residues such as Leu_{21} or Leu_{24} are converted to Gly, there is complete elimination of the PDBU binding capability, and this cannot be attributed entirely to changes in PKC−lipid interaction because in the absence of lipid the PDBU binding affinity is not eliminated but reduced by a factor of 80.[43] Rather, this must indicate that the conformation of the 21−27 loop is changed as a result of either mutation. The extreme sensitivity to mutation of the residues in this loop testifies eloquently against the validity of model A, which does not involve any residues in the 21−27 loop.

It is possible that the *ca*. 50-fold loss in PDBU binding affinity of the protein caused by the mutation of Tyr_8 to Gly might be entirely due to the decrease in protein−lipid association, but in the case of the more than 100-fold decrease in the protein's ability to bind to PDBU when Pro_{11} is mutated to Gly, other factors should also play a role. In fact, this decrease in the PDBU/PKC binding affinity may reflect the importance to enzyme−ligand interactions of the backbone conformation of the loop formed by residues 6−13. This speaks against model B as the correct model for PKC/PDBU binding.

Thus the site-directed mutagenesis data support model C and suggest that both the 6−13 and 21−27 loops are involved in the PKC/PDBU binding. The important role played by Thr_{12} in the binding is of special interest. Although the main contribution from Thr_{12} comes from its backbone interactions with the hydrogen group at C_{20} in PDBU (model C), the amino acid side chain of Thr_{12} also contributes *ca*. 2 kcal/mol of hydrogen bond energy and therefore is important to the PKC/PDBU binding. Mutation to Gly of this residue however gives only about a 2-fold decrease in the binding affinity, smaller than predicted by model C. A molecular modeling study designed to investigate the interactions between PDBU and this mutant showed that while the hydrogen bond from the Thr_{12} side chain is lost, there is in the mutant a new hydrogen bond between the C_{20} hydroxyl in PDBU and Ser_{10}, and the total hydrogen bond energy between the mutant PKC and PDBU in model C is only about 0.5 kcal/mol smaller than that between the wild-type PKC_α and PDBU. This explains the experimental mutagenesis results and provides further support for model C.

Molecular Dynamics Simulation of the X-ray-Determined Structure. While this work was in progress, the structure of the complex formed between phorbol 13-acetate and PKC_δ was solved.[36] This allows molecular modeling studies of the X-ray-determined complex and direct comparisons with our modeling results.

The X-ray-determined structure was placed in a shell of 500 water molecules and minimized. Hydrogen bonds are formed between phorbol 13-acetate and PKC_δ in the X-ray-determined, energy-minimized structure as shown in Figure 7. In this structure, the phorbol ester interacts with the protein by means of hydrogen bonds with the oxygen atoms at C_3, C_4, and C_{20}. Specifically, the oxygen at C_3 forms a strong hydrogen bond with the NH of Gly_{23}, the hydroxyl group at C_4 interacts with the carbonyl of Gly_{23} through a strong hydrogen bond and with the side chain of Gln_{27} through a weak hydrogen bond, and the hydroxyl group at C_{20}, being both an acceptor and a donor, forms two strong hydrogen bonds with the NH of Thr_{12} and the carbonyl of Leu_{21}.

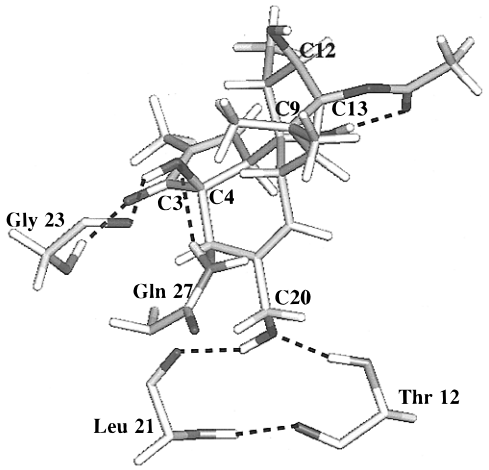

Figure 7. Hydrogen bonds between PKC$_\delta$/phorbol 13-acetate in the X-ray-determined structure.

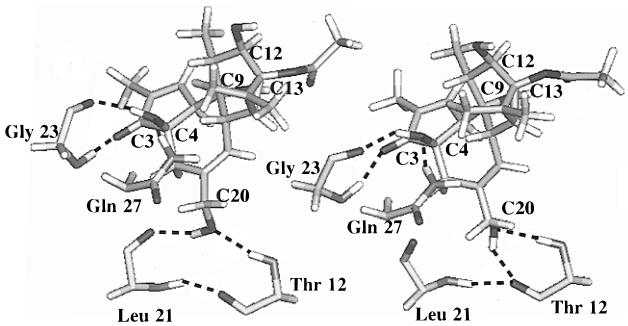

Figure 8. Molecular dynamics simulation trajectories of the X-ray-determined structure.

To further investigate the stability of the X-ray structure, 150 ps of molecular dynamics simulation was performed on the complex in the water shell at 300 K. No constraints were used other than on the eight bonds to the zinc atoms of the two zinc fingers. Snapshots were taken at $t = 0$ and at 10 ps intervals, and each of the resulting structures was minimized in the water environment. Two snapshots at 50 and 100 ps of the simulation are shown in Figure 8. The results, presented in Table 7, revealed the entire structure to be stable with an overall hydrogen bond energy (−11.28 ± 1.68 kcal/mol) which did not change appreciably during the dynamics simulation. Throughout the complete simulation, the only hydrogen bonds formed between the ligand and the protein were those involving the oxygen atoms at C_3, C_4, and C_{20} of the phorbol ester. The oxygens at C_9, C_{12}, and C_{13} appear to play no part in hydrogen bonding to the protein. A strong intramolecular hydrogen bond between the C_9 hydroxyl and the carbonyl oxygen at C_{13} is retained in all the trajectories. The C_3 oxygen forms a strong hydrogen bond with the backbone NH of Gly_{23}, while the C_4 hydroxyl group in the ligand forms a strong hydrogen bond with the backbone carbonyl group of Gly_{23} and a weak bond with the side chain amino group of Gln_{27}. It is noted that the hydrogen bonds formed between the hydroxyl at C_4 and the protein are not optimal in the X-ray-derived structure, and their strength improves during the molecular dynamics simulation. The C_{20} hydroxyl group is the most important binding point in the ligand, binding to the backbone NH of Thr_{12} and the backbone carbonyl of either Leu_{21} or Thr_{12}. Hydrogen bonds

Table 7. Summary of the Total Hydrogen Bond Energy (kcal/mol) between 12-Hydroxyphorbol 13-Acetate and PKC$_\delta$ for a Total of 15 Minimized Structures That Were Obtained from 150 ps Molecular Dynamics Simulations in Water Started with the X-ray-Determined Complex Structure and the Hydrogen Bond Energy Contributed from Each of the Binding Elements in 12-Hydroxyphorbol 13-Acetate

simulation time (ps)	total HB energy	HB energy between PKC$_\delta$ and specific phorbol 13-acetate atoms		
		C_3 O	C_{20} OH	C_4 OH
10	−11.47	−3.33	−5.59	−2.55
20	−12.06	−2.96	−5.72	−3.38
30	−12.44	−1.81	−4.29	−6.35
40	−11.10	−1.45	−6.28	−3.38
50	−13.69	−3.04	−6.06	−4.59
60	−10.53	−1.79	−6.79	−1.95
70	−11.10	−3.29	−6.12	−1.69
80	−14.40	−3.38	−6.93	−4.09
90	−11.37	−3.20	−3.59	−4.58
100	−12.52	−2.20	−5.25	−5.08
110	−10.81	−2.01	−5.90	−2.91
120	−9.55	−2.99	−1.75	−4.80
130	−9.17	−2.78	−4.37	−2.01
140	−11.27	−3.47	−3.06	−4.74
150	−7.81	−2.15	−3.40	−2.27
		average		
	−11.28	−2.66	−5.01	−3.62
		SD		
	1.68	0.68	1.52	1.39

involving the C_{20} hydroxyl contribute −5.01 kcal/mol, some 44%, to the total hydrogen bond energy of the complex.

In the complex formed by PKC$_\delta$ and phorbol 13-acetate then, the oxygens at C_3, C_4, and C_{20} of the ligand are responsible for most of the binding, the corresponding residues in the protein being Gly_{23}, Gln_{27}, Thr_{12}, and Leu_{21} (or Thr_{12}).

There are marked similarities between the binding revealed by this X-ray structure and our model C. Both models agree that the C_{20} hydroxyl is of primary importance in the binding and that the C_3 carbonyl also plays a significant role. These two ligand-binding points together account for 65−75% of the total hydrogen-bonding energy. A major difference between the models concerns the hydroxyl at C_4. Its role in model C is minimal, contributing only −0.36 kcal/mol to the total hydrogen-bonding energy, but in the X-ray model it contributes −3.62 kcal/mol. Likewise, the X-ray model showed the carbonyl at C_{13} to be intramolecularly hydrogen bonded to the hydroxyl at C_9 and uninvolved in protein binding. Model C, on the other hand, has the C_9 hydroxyl (−0.76 kcal/mol) and, especially, the C_{13} carbonyl hydrogen (−3.28 kcal/mol) bonded to the protein with a total energy of −4.04 kcal/mol—23% of the total hydrogen-bonding energy. Thus while the two models agree on the major points, there are discrepancies, and these will be discussed in the next section.

Discrepancies between Model C and the X-Ray Model. Model C was based upon the NMR-determined solution structure of PKC$_\alpha$, while the X-ray model was of the crystal structure of PKC$_\delta$, and some of the discrepancies may derive from the different nature of the measurement processes. Comparisons of the two models reveal some interesting differences in the protein structures. Both models agree that the active site involves two loops, from His_6 to Phe_{13} and Leu_{20} to Gln_{27}. In the NMR structure, shown on the left side of Figure 9, which was used to derive model C, the active

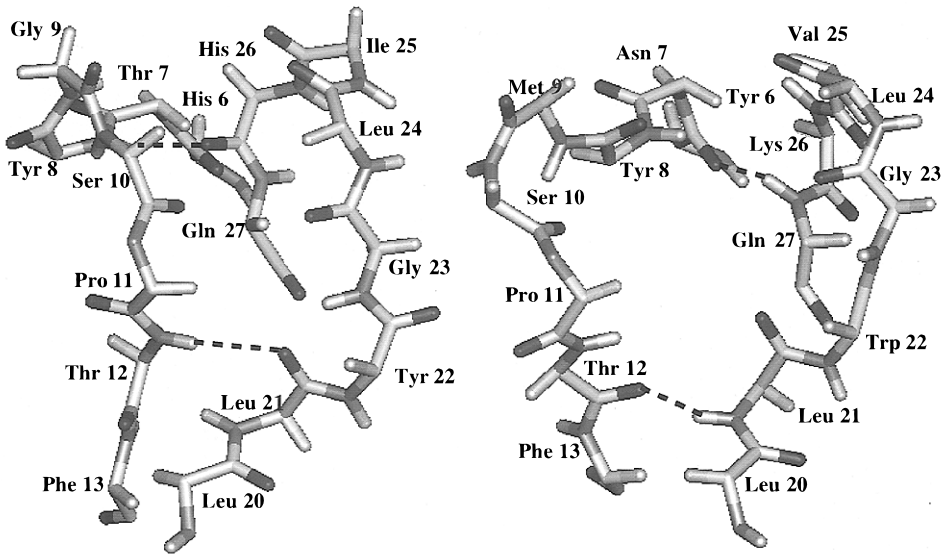

Figure 9. Comparisons of the NMR-determined solution structure of PKC_{α} and the X-ray-determined solid state structure of PKC_{δ}.

site is constrained by two hydrogen bonds, formed between the NH of Thr_{12} and the carbonyl of Leu_{21} and between the NH of Tyr_8 and the carbonyl of His_{26}. In the X-ray structure, shown on the right side of Figure 9, however, the first of these two hydrogen bonds is formed between the carbonyl of Thr_{12} and the NH of Leu_{21}, but the second is replaced by a hydrogen bond between the carbonyl of Tyr_6 and the backbone NH of Gln_{27}. The result is that the loops have different lengths in the two models. The two loops are nine residues in length in the NMR-determined structure but 12 residues in length in the X-ray structure. This is the major difference between the two structures and underlies all the detailed differences between model C and the X-ray model.

It is noteworthy that neither of these binding modes appears to be converted to the other during 150 ps dynamics simulations at 300 K. Simulations at higher temperatures were not carried out, but this suggests that both structures are discrete entities and that there is at least a nominal energy barrier between them.

Discussion

In a recent review of the PKC problem,[44] the importance of the X-ray data was pointed out and various questions that arise from the X-ray study were raised. First, the PKC_{δ}−phorbol 13-acetate complex that was analyzed was prepared in the absence of any lipid. Lipid is known to be involved in the natural binding process, and its presence may affect the structure of the resulting complex. Second, the ligand used, phorbol 13-acetate, was chosen for its aqueous solubility but actually binds only very weakly to PKC. A ligand like PDBU binds 4 orders of magnitude more strongly to the enzyme, corresponding to an energy difference of about 5.5 kcal/mol, raising the possibility that a different binding mode may be operating. Third, the X-ray data reflect the structure in the solid state which may well be different in detail from that measured by NMR in solution.

There are also *caveats* that should not be overlooked with respect to the modeling studies. First, all these were performed in the absence of lipid, and any effect lipid might have would be missed. Second, the modeling studies used a previously defined pharmacophore model, a choice which might bring some bias to the modeling, although it should be pointed out that the binding site that emerges from the modeling studies is in fact the same as that derived from the X-ray model. Third, the modeling used the NMR-derived structure of PKC_{α} as a starting point, and any uncertainties in the NMR data will have been carried forward. Indeed, the disordering, in the NMR data, of part of the structure has already been remarked upon. Finally, we have used hydrogen-bonding energy as the major marker of binding, although we are cognizant of the fact that other forces such as hydrophobic interactions may also play an important role in binding.

In summary, we have two structures for a ligand bound to PKC. They have great similarities but also some differences, which may arise from any of several known differences in the methodology of determination, as detailed above. Since there is a high level of agreement between them, it seems safe to conclude that both the structures should be useful as models for PKC binding.

Conclusion

Molecular modeling studies of the structures of the complexes formed between different PKC ligands and the second cysteine-rich domain of PKC_{α} have allowed us to develop a binding model for phorbol esters and DAG, in which the precise nature of the binding of the ligands to the enzyme is defined. The site of the binding model is supported by site-directed mutagenesis results and consistent with the X-ray-determined PKC/phorbol ester structure. Both models were found stable in molecular dynamics simulations. However, the precise binding elements in phorbol esters in these two models determined through X-ray and modeling are not identical. In the X-ray model, the oxygens at C_3, C_4, and C_{20} in phorbol esters were shown to be involved in the protein/ligand interactions and form hydrogen bonds with the backbone of the protein. In the modeling-derived model, the oxygens at C_3, C_{13}, and C_{20} in phorbol esters were found to play primary roles to the binding, while the oxygen at C_9 plays a complementary role and the oxygen at C_4 is of minimal significance to the

binding. The two models identified that the most important binding element in phorbol esters is the oxygen at C_{20} and the oxygen at C_3 plays an important role in the binding. As for the roles of the oxygens at C_4, C_9, and C_{13} in phorbol esters for the binding, it appears that the modeling-derived model is more consistent with the known structure−activity data of phorbol esters, while the X-ray model would suggest somewhat different results. The X-ray and modeling results also differ on the residues in PKC that are involved in the phorbol ester binding. This is probably due to the discrepancies between the NMR-determined solution structure and X-ray-derived solid state structure for PKC with respect to the binding region, the loop formed by residues 6−12 and 21−27.

It is possible that PKC ligands with low and high binding affinities bind to the same binding site but with somewhat different binding modes or that the same ligand binds to PKC in different environments because the NMR-determined solution structure of the second cysteine-rich domain is, with respect to the binding region, different from the X-ray-determined solid state structure. In addition, due to the lack of phospholipid and the use of a low-binding-affinity ligand in the X-ray study, as well as the differences between our modeling-derived and the X-ray-determined binding modes for phorbol esters, further studies are therefore necessary in order to fully address how phorbol esters bind to PKC in the PKC−phospholipid−ligand aggregate.

Our present studies, combining molecular modeling and site-directed mutagenesis, illustrate a general and effective approach to not only pinpoint the binding site on protein for ligands but also predict the precise nature of the binding. Both the modeling and the X-ray results shed light on the binding of tumor promoters to PKC and provide us with an opportunity to study how other classes of tumor promoters and PKC ligands, such as teleocidins, ingenols, aplysiatoxins, and bryostatins, bind to PKC. They also pave the way for the structure-based design of novel PKC ligands.

Acknowledgment. We would like to thank Dr. Ulrich Hommel of Sandoz for providing us the coordinates of the second zinc finger in PKC_α, determined by NMR, and Dr. James Hurley of NIDDK, NIH, for the coordinates of the second zinc finger of PKC_δ, determined by X-ray diffraction. Both sets of coordinates were provided to us prior to deposition into the Brookhaven Protein Data Bank.

References

(1) Nishizuka, Y. The Role of Protein Kinase C in Cell Surface Signal Transduction and Tumor Promotion. *Nature* **1984**, *308*, 693−698.
(2) Nishizuka, Y. Studies and Perspectives of Protein Kinase C. *Science* **1986**, *233*, 305−312.
(3) Nishizuka, Y. The Molecular Heterogeneity of Protein Kinase C and its Implications for Cellular Regulation. *Nature* **1988**, *334*, 661−668.
(4) Bell, R. M. Protein Kinase C Activation by Diacylglycerol Second Messengers. *Cell* **1986**, *45*, 631−632.
(5) Weinstein, I. B. The Origin of Human Cancer: Molecular Mechanisms of Carcinogenesis and their Implications for Cancer Prevention and Treatment. *Cancer Res.* **1988**, *48*, 4135−4143.
(6) Rahmsdorf, H. J.; Herrlich, P. Regulation of Gene Expression by Tumor Promoters. *Pharmacol. Ther*. **1990**, *48*, 157−188.
(7) Berridge, M. Inositol Triphosphate and Diacylglycerol: Two Interacting Second Messengers. *Annu. Rev. Biochem*. **1987**, *56*, 159−193.
(8) Blumberg, P. M. Protein Kinase C as the Receptor for the Phorbol Ester Tumor Promoters. Sixth Rhoads Memorial Lecture. *Cancer Res.* **1988**, *48*, 1−8.
(9) Jeffrey, A. M.; Liskamp, R. M. J. Computer-assisted Molecular Modeling of Tumor Promoters: Rationale for the Activity of Phorbol Esters, Teleocidin B and Aplysiatoxin. *Proc. Natl. Acad. Sci. U.S.A.* **1986**, *83*, 241−245.
(10) Wender, P. A.; Koehler, K. G.; Sharkey, N. A.; Dell'Aquila, M. L.; Blumberg, P. M. Analysis of the Phorbol Ester Pharmacophore on Protein Kinase C as a Guide to the Rational Design of New Classes of Analogs. *Proc. Natl. Acad. Sci. U.S.A.* **1986**, *83*, 4214−4218.
(11) Itai, A.; Kato, Y.; Tomioka, N.; Endo, Y.; Hasegawa, M.; Shudo, K.; Fujiki, H.; Sakai, S. A Receptor Model for Tumor Promoters: Rational Superposition of Teleocidins and Phorbol Esters. *Proc. Natl. Acad. Sci. U.S.A.* **1988**, *85*, 3688−3692.
(12) Wender, P. A.; Cribbs, C. M.; Koehler, K. G.; Sharkey, N. A.; Herald, C. L.; Kamano, Y.; Pettit, G. R.; Blumberg, P. M. Modeling of the Bryostatins to the Phorbol Ester Pharmacophore on Protein Kinase C. *Proc. Natl. Acad. Sci. U.S.A.* **1988**, *85*, 7197−7201.
(13) Nakamura, H.; Kishi, Y.; Pajares, M. A.; Rando, R. R. Structural Basis of Protein Kinase C Activation by Tumor Promoters. *Proc. Natl. Acad. Sci. U.S.A.* **1989**, *86*, 9672−9676.
(14) Kong, F.; Kishi, Y.; Perez-Sala, D.; Rando, R. R. The Pharmacophore of Debromoaplysiatoxin Responsible for Protein Kinase C Activation. *Proc. Natl. Acad. Sci. U.S.A.* **1991**, *88*, 1973−1976.
(15) Hommel, U.; Zurini, M. Solution Structure of a Cysteine Rich Domain of Rat Protein Kinase C. *Nature Struct. Biol.* **1994**, *1*, 383−387.
(16) Ichikawa, S.; Hatanaka, H.; Takeuchi, Y.; Ohno, S.; Inagaki, F. Solution Structure of Cysteine-Rich Domain of Protein Kinase Cα. *J. Biochem*. **1995**, *117*, 566−574.
(17) Quest, A. F. G.; Bardes, E. S. G.; Bell, R. M. A Phorbol Ester Binding Domain of Protein Kinase Cγ. Deletion Analysis of the cys2 Domain Defines a Minimal 43-Amino Acid Peptide. *J. Biol. Chem*. **1994**, *269*, 2961−2970.
(18) The second cysteine-rich domain of PKC_α ($His_{102} \rightarrow Cys_{152}$) is the subject of this paper, and for the sake of discussion, it has been renumbered as shown in Figure 1. Thus His_{102} is now His_1, and Cys_{152} is now Cys_{50}.
(19) QUANTA/CHARMm, a molecular modeling system, is supplied by Molecular Simulations Inc., 200 Fifth Ave., Waltham, MA 01803-5279.
(20) Brooks, B. R.; Bruccoleri, R. E.; Olafson, B. D.; States, D. J.; Swaminathan, S.; Karplus, M. CHARMm: A Program for Macromolecular Energy, Minimization, and Dynamics Calculations. *J. Comput. Chem*. **1983**, *4*, 187−217.
(21) Teng, K.; Marquez, V. E.; Milne, G. W. A.; Barchi, J. J.; Kazanietz, M. G.; Lewin, N. E.; Blumberg, P. M.; Abushanab, E. A. Conformationally Constrained Analogs of Diacylglycerol. Interaction of γ-Lactones with the Phorbol Ester Receptor of Protein Kinase C. *J. Am. Chem. Soc.* **1992**, *114*, 1059−1070.
(22) Kazanietz, M. G.; Wang, S.; Milne, G. W. A.; Lewin, N. E.; Liu, H. L.; Blumberg, P. M. Residues in the Second Cysteine-rich Region of Protein Kinase C δ Relevant to Phorbol Ester Binding As Revealed by Site-Directed Mutagenesis. *J. Biol. Chem*. **1995**, *270*, 21852−21859.
(23) Ono, Y.; Fujii, T.; Igarashi, K.; Kuno, T.; Tanaka, C.; Kikkawa, U.; Nishizuka, Y. Phorbol Ester Binding to Protein Kinase C Requires a Cysteine-rich Zinc Finger-like Sequence. *Proc. Natl. Acad. Sci. U.S.A.* **1989**, *86*, 3099−3103.
(24) Quest, A. F.; Bloomenthal, J.; Bardes, E. S.; Bell, R. M. The Regulatory Domain of Protein Kinase C Coordinates Four Atoms of Zinc. *J. Biol. Chem*. **1992**, *267*, 10193−10197.
(25) Burns, D. J.; Bell, R. M. Protein Kinase C Contains Two Phorbol Ester Binding Domains. *J. Biol. Chem*. **1991**, *266*, 18330−18338.
(26) Quest, A. F. G.; Bardes, E. S. G.; Bell, R. M. A Phorbol Ester Binding Domain of Protein Kinase C gamma. High Affinity Binding to a Glutathione-S-transferase/Cys2 Fusion Protein. *J. Biol. Chem*. **1994**, *269*, 2953−2960.
(27) Kazanietz, M. G.; Bustelo, X. R.; Barbacid, M.; Mischak, H.; Kolch, W.; Wong, G.; Pettit, G. R.; Bruns, J. D.; Blumberg, P. M. Zinc Finger Domains and Phorbol Ester Pharmacophore. Analysis of Binding to Mutated Form of Protein Kinase C zeta and the vav and c-raf Proto-oncogene Products. *J. Biol. Chem*. **1994**, *269*, 11590−11594.
(28) Wender, P. A.; Irie, K.; Miller, B. L. Identification, Activity, and Structural Studies of Peptides Incorporating the Phorbol Ester-binding Domain of Protein Kinase C. *Proc. Natl. Acad. Sci. U.S.A.* **1995**, *92*, 239−243.
(29) Kazanietz, M. G.; Areces, L. B.; Bahador, A.; Mischak, H.; Goodnight, J.; Mushinski, J. F.; Blumberg, P. M. Characterization of Ligand and Substrate Specificity for the Calcium-dependent and Calcium-independent PKC Isozymes. *Mol. Pharmacol*. **1993**, *44*, 298−307.
(30) Quest, A. F. G.; Bardes, E. S. G.; Bell, R. M. A Phorbol Ester Binding Domain of Protein Kinase C gamma. Deletion Analysis of the Cys2 Domain Defines a Minimum 43-amino Acid Peptide. *J. Biol. Chem*. **1994**, *269*, 2961−2970.
(31) Kazanietz, M. G.; Blumberg, P. M. Unpublished results.
(32) Scott, D. L.; White, S. P.; Otwinowski, Z.; Yuan, W.; Gelb, M. H.; Sigler, P. B. Interfacial Catalysis: The Mechanism of Phospholipase A_2. *Science* **1990**, *250*, 1541−1546.

(33) Sugita, K.; Neville, C. F.; Sodeoka, M.; Sasai, H.; Shibasaki, M. Stereocontrolled Syntheses of Phorbol Analogs and Evaluation of their Binding Affinity to PKC. *Tetrahedron Lett.* **1995**, *36*, 1067−1070.
(34) Hecker, E. Cell Membrane Associated Protein Kinase C as Receptor of Diterpene Ester Co-carcinogens of the Tumor Promoter Type and the Phenotype Expression of Tumors. *Arzneim.-Forsch/Drug Res.* **1985**, *35*, 1890−1903.
(35) Wang, S.; Milne, G. W. A.; Nicklaus, M. C.; Marquez, V. E.; Lee, J.; Blumberg, P. M. Protein Kinase C. Modeling of the Binding Site and Prediction of Binding Constants. *J. Med. Chem.* **1994**, *37*, 1326−1338.
(36) Zhang, G.; Kazanietz, M. G.; Blumberg, P. M.; Hurley, J. H. Crystal Structure of the Cys2 Activator Binding Domain of Protein Kinase C delta in Complex with Phorbol Ester. *Cell* **1995**, *81*, 917−924.
(37) A 1100-fold difference in binding affinity corresponds to *ca.* 4.2 kcal/mol, neglecting entropy.
(38) Boni, L. T.; Rando, R. R. The Nature of Protein Kinase C Activation by Physically Defined Phospholipid Vesicles and Diacylglycerols. *J. Biol. Chem.* **1985**, *260*, 10819−10825.
(39) Young, N.; Rando, R. R. The Sterospecific Activation of Protein Kinase C. *Biochem. Biophys. Res. Commun.* **1984**, *122*, 818−823.
(40) Smith, S. O.; Kustanovich, I.; Bhamidipati, S.; Salmon, A.; Hamilton, J. A. Interfacial Conformation of Dipalmitoylglycerol and Dipalmitoylphosphatidylcholine in Phospholipid Bilayers. *Biochemistry* **1992**, *31*, 11660−11664.
(41) Lewin, N. E.; Blumberg, P. M. Unpublished observations.
(42) Sugita, K.; Neville, C. F.; Sodeoka, M.; Sasai, H.; Shibasaki, M. Stereocontrolled Syntheses of Phorbol Analogs and Evaluation of their Binding Affinity to PKC. *Tetrahedron Lett.* **1995**, *36*, 1067−1070.
(43) Kazanietz, M. G.; Barchi, J. J., Jr.; Omichinski, J. G.; Blumberg, P. M. Low Affinity Binding of Phorbol Esters to Protein Kinase C and its Recombinant Cysteine-Rich Region in the Absence of Phospholipids. *J. Biol. Chem.* **1995**, *270*, 14679−14684.
(44) Rouhi, A. M. Crystal structure sheds light on binding of tumor promoters to key enzyme. *C&EN* **1995**, October, 21−25.

JM950403N